Structural organization of fibrous connective tissue in the periacinar region of the transitional zone from normal human prostates as revealed by scanning electron microscopy

Márcio A. Babinski, Waldemar S. Costa, Francisco J.B. Sampaio and Luiz E.M. Cardoso

Urogenital Research Unit, State University of Rio de Janeiro, Rio de Janeiro, RJ, Brazil

OBJECTIVE

To analyse, using scanning electron microscopy (SEM), the organization of stromal fibrous components in the transitional zone (TZ) from normal human prostates; because of its association with disease, greater emphasis was placed upon the periacinar region of the stroma.

MATERIALS AND METHODS

TZ specimens were obtained from normal prostates during autopsy of six men, aged 18–30 years, who had died from accidents. Tissue was fixed for SEM in a modified Karnovsky solution for 48 h at 4 °C, and to visualize the three-dimensional organization of the stroma, samples were treated to remove cells.

RESULTS

In acellular preparations, narrow fibrous septa formed a dense and supportive scaffold for ducts and acini, and a smooth and homogeneous fibrous sheet, herein identified as pars fibroreticularis, lined the acinar lumen. More internally, fibrous septa had a spongy organization with dense lamellae. Higher magnification showed that the smooth luminal sheet is made of 115–154-nm thick fibrils in a tight parallel arrangement. Just under this layer there was a meshwork of fibrils 77–115 nm thick that were orientated in less defined directions.

CONCLUSION

In the TZ of the human prostate, dense stromal fibrous components around acini act as a barrier that might enhance local cellular responses and events that occur in disorders such as benign prostatic hyperplasia. The periacinar pars fibroreticularis supports the notion of high structural variability in this region of basement membranes.

KEYWORDS

prostate stroma, prostate transitional zone, connective tissue, scanning electron microscopy

INTRODUCTION

The transitional zone (TZ) is particularly relevant for prostate pathology as it is thought to be the main region of the gland which enlarges in BPH [1]. This urological disorder, the commonest in men aged ≥50 years [2], is associated with complex and not well understood interactions between acinar epithelial cells and their supportive stroma. Several autocrine and paracrine stimuli are involved in these interactions, which ultimately modulate cell proliferation and the expression of stromal extracellular matrix molecules [3]. Epithelial–stromal interactions and stromal extracellular matrix (ECM) components also play key roles in normal prostate physiology and in tumour growth [4,5]. However, ECM turnover during tumour development can vary according to prostate region, as the TZ expresses fewer metalloproteinases than the peripheral zone [6]. Studies on the pathophysiology of prostate disorders should therefore consider these heterogeneous cellular responses and focus the analyses on specific regions of the gland. This approach is further warranted by findings showing that the different zones of the normal gland have distinct histological and physiological features [7–9]. Therefore, to properly evaluate changes in a given region of the prostate, the control that should be used is the corresponding region of the normal gland. Indeed, if comparisons are not made against these controls, any interpretation or results might be erroneous [9].

By using immunohistochemistry we showed that the expression of chondroitin sulphate proteoglycans is selectively greater in the periacinar stroma of the hyperplastic prostate than in the normal TZ [10], and other morphological techniques indicate that elastic and reticular fibres might also be increased in this disease, using similar controls [11]. Because chondroitin sulphate proteoglycans have been implicated in cell growth, migration and transformation [12], the ECM surrounding acini, including its basement membrane, might have a pivotal role in the proliferative responses that accompany prostate disorders. Indeed, it was shown recently that perlecan, a basement membrane proteoglycan, binds growth factors that directly affect the metastatic phenotype of prostate cells [13]. Despite this evidence showing the importance of the ECM and of the internal glandular heterogeneity, there are few studies on the ultrastructural organization of the human prostatic stroma [14,15], of which none has specifically analysed the TZ and its periacinar region. Thus, little is known about the normal morphological organization of the connective tissue in this critical portion of the prostate.

In the present study we used scanning electron microscopy (SEM) to analyse the three-dimensional organization of the fibrous

FIG. 1. Periacinar region of the TZ of the prostate (asterisk) as seen in a routine preparation for light microscopy. A, lumen of acinus. Haematoxylin and eosin; original ×400; the scale bar represents 10 μm.
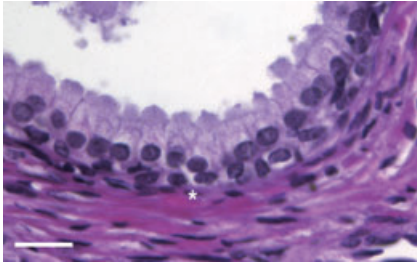

FIG. 2. Periacinar region of the TZ in an intact prostate sample examined under low-vacuum SEM. In this preparation the epithelial cells (E), stromal septa (asterisk) and ducts (D) are visible. Epithelial cells are well preserved and their apical poles, as seen from the acinar lumen, have a 'cobblestone' arrangement. Original ×400; the scale bar represents 30 μm.
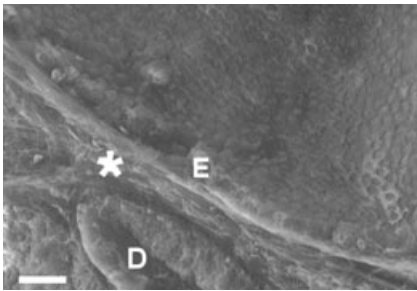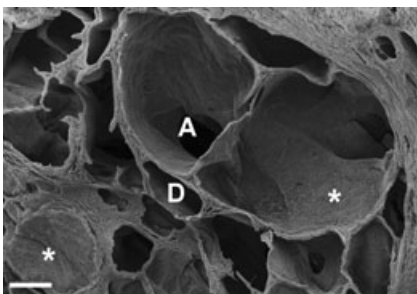

FIG. 3. Acini and surrounding stroma in an acellular preparation of the TZ of the prostate as seen under high-vacuum SEM. Note the smooth luminal surface (asterisks) lining the empty acinar spaces (A). D, duct. Original ×150; the scale bar represents 200 μm.

components in the stroma of the TZ from normal human prostates. Because it is often associated with prostatic disease, greater emphasis was placed upon the periacinar region of the stroma. Our samples were obtained from young adults and consisted of intact tissue and alkali-treated acellular preparations.

MATERIALS AND METHODS

The Ethics Committee on Human Research of the State University of Rio de Janeiro reviewed and approved this study. TZ specimens were obtained during autopsy from six men (mean age 24 years, SD 4.0, range 18–30) who had died as a results of accidents. The prostates were macroscopically normal and the mean (SD, range) weight of the whole gland was 15.0 (2.6, 12.0–19.0) g. The TZ was located and dissected, as previously described [1,16], and tissue specimens from it were immediately placed in a fixative solution. The time elapsed between death and fixation of the samples was <8 h.

Fixation for SEM was done by immersing tissue fragments in a modified Karnovsky solution for 48 h at 4 °C; the fixative consisted of 2.5% glutaraldehyde and 2% paraformaldehyde in 0.1 M sodium phosphate buffer, pH 7.4. Part of the tissue specimens was routinely processed for paraffin embedding, and the 5-μm thick sections were stained with haematoxylin/eosin and examined by a pathologist not involved in the study, to detect and exclude foci of carcinoma or BPH.

To better visualize the three-dimensional organization of the prostatic stroma under SEM, tissue samples were treated to solubilize and remove cells [17]. Thus, for each man, about three fixed TZ fragments (1 × 1 cm) were washed in PBS for 2 h at 4 °C and then incubated in 40 mL of 2 M NaOH at room temperature for 8 days. The samples were then rinsed in three changes of 24 h each in 40 mL of distilled water at room temperature, until they were pale and transparent.

The processing of materials for high-vacuum SEM followed standard procedures [17]. Accordingly, acellular preparations were first treated with 1% tannic acid in PBS for 2 h and washed in PBS for 1 h. Post-fixation was done in 1% osmium tetroxide in PBS for 3 h, after which the samples were washed in PBS for 1 h and dehydrated in an ascending graded series of ethanol. Samples were then critical-point dried with liquid carbon dioxide, mounted on aluminium stubs with carbon

cement, and coated with gold using a sputter coater. The samples were examined in a SEM with an acceleration voltage of 15–20 kV. To better characterize stromal fibrous components and allow comparison against other tissues, approximate linear thickness was measured on calibrated digital photographs taken at × 8000 and using the program ImageJ version 1.37 (National Institutes of Health, Bethesda, Maryland, USA). The measurements were made on ≈30 fibrous elements per individual in at least five different fields.

Intact samples, which consisted of fixed but otherwise unprocessed tissue specimens, were also examined directly under low-vacuum SEM to assess the luminal surface of the acinar epithelium and the overall quality of the sample. This SEM technique was also used to monitor the efficiency and extent of the cellular solubilization process. All descriptive data are representative of the six prostate samples used in this study.

RESULTS

Routinely prepared histological sections of the TZ from the six prostate samples showed that the periacinar stroma consists of dense fibrillar bundles interspersed with fusiform cells. These stromal components were mostly distributed in concentric layers around the luminal surface of the acinus and were in close apposition to the basal epithelial cells thereof (Fig. 1). Observation of this region using low-vacuum SEM and intact tissue samples showed a well-preserved acinar epithelium and revealed that the stroma surrounding ducts and acini is structured as a framework of septa (Fig. 2).

To investigate in greater detail the three-dimensional organization of this framework, and especially of its constituent connective tissue, prostate samples were treated with a 2 M NaOH solution, which solubilizes cells, and were then examined under high-vacuum SEM. These acellular preparations showed that relatively narrow fibrous septa form a dense and supportive scaffold for ducts and acini (Figs 3–5). Also, removing the epithelial cells showed that a smooth and grossly homogeneous fibrous sheet lines the surface of the empty acinar spaces (Fig. 3). However, the more internal or deeper ECM of fibrous septa, as seen in transverse sections, had a spongy organization with thin but dense

lamellae delimiting empty spaces which were formerly occupied by cells (Figs 4 and 5). Projections from the septa into the luminal space were evident in some acini (Fig. 4).

The smooth luminal sheet is a thin fibrous structure that is closely adherent to the lamellae of the septa (Figs 4 and 5). In addition, higher magnification showed that this smooth sheet actually consists of different structural components forming distinct layers. The inner layer, which directly faces the empty acinar space, is smoother and made of 115–154-nm thick fibrils that are tightly arranged parallel to one another, to form a sheet (Fig. 6). Just under this layer there is a meshwork of loosely woven thin fibrils, of 77–115 nm thick, that are orientated in less defined directions (Figs 6 and 7).

DISCUSSION

It is well established that the different macromolecules of the ECM combine in various compositions and/or proportions to form connective tissues that vary widely in morphological structure and function. In the human prostate, investigations using different methods showed that the stromal ECM contains collagen types I, III, IV and V, fibronectin, laminin, chondroitin sulphate and heparan sulphate proteoglycans, and elastic fibrrs [10,11,18]. This composition is thought to be highly organ-specific [19], and factors from the prostate stroma can, indeed, induce non-prostate epithelial cells to differentiate into a prostatic phenotype [20].

Although apparently homogeneous under light microscopy, the prostate stromal ECM around acini is organized as different structures, e.g. fibrous sheets and spongy septa that are made up of dense lamellae, as was particularly evident in the present acellular preparations. The distinct conformations and locations of these structures imply different functions, e.g. supportive scaffold, retention of soluble factors, and regulation of diffusion [21], which should result from locally different proportions of ECM molecular components. The stroma of the TZ of the normal human prostate should therefore be spatially heterogeneous. Moreover, this condition, which facilitates the formation of micro-environments, might be enhanced in disease. For example, a SEM investigation on the density of collagen fibres in the prostatic

stroma as a whole showed differences among normal, hyperplastic and malignant tissues, although the anatomical locations of the samples that were examined were not indicated [15]. Also, in BPH the stromal distribution of cytokines differs from that in the normal gland [22], while the periacinar and interstitial stroma in this disease have markedly distinct ECM compositions [10].

Interestingly, this latter finding can be explained by our results on the three-dimensional organization of the normal prostate stroma. In BPH, acinar epithelial cells are known to release growth factors and cytokines that can exert various effects on stromal cells, including enhanced synthesis of ECM molecules [3,23]. These paracrine effects depend on diffusion of the factors from the acinar epithelium to the stromal cells through the ECM, which itself acts as a barrier to such diffusion [21]. As stromal lamellae surrounding acini contain elastic fibres [11] and are composed of dense connective tissue, as shown in the present results, diffusion of factors would be more limited, and only stromal cells that are more adjacent to the epithelium should be affected. Our previous findings therefore support this hypothesis, as we showed that in BPH the expression of chondroitin sulphate proteoglycans is selectively and conspicuously increased in the periacinar region, with little or no labelling in the remainder of the stroma, compared with the TZ of the normal prostate [10]. A denser matrix also makes it more difficult for cells to migrate [24] and as such might contribute to the nodular organization of stromal smooth muscle cells in BPH [25].

FIG. 4. Transversely sectioned stromal septum (star) between acini (A). Note the spongy organization of the stromal ECM and the projections from the stroma (asterisk) into the acinar lumen. Frames a and b are shown at higher magnification in Figs 5 and 7, respectively. Original ×500; the scale bar represents 40 μm.
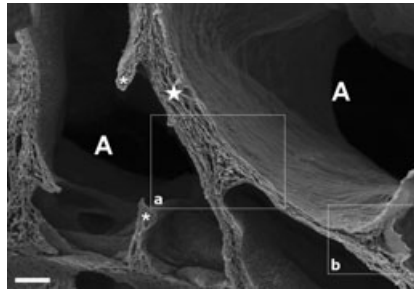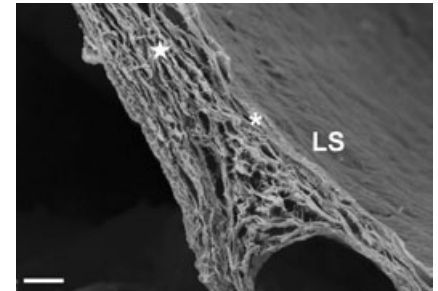

FIG. 5. Higher magnification of Fig. 4a showing the inner structure of a stromal septum (star). The spongy organization of the septum results from the presence of dense fibrous lamellae and empty cellular spaces. The luminal sheet (LS) lining the empty acinus has a relatively smooth surface and is closely adherent to the underlying stroma (asterisk). Original ×1500; the scale bar represents 20 μm.

FIG. 6. Luminal sheet lining the empty acinar space. The higher magnification shows that the luminal sheet is composed of fibrils in a parallel arrangement. In places where these fibrils are more widely separated, a meshwork of 115–154-nm thick fibrils forming a layer just underneath is visible (arrow). Original ×8000; the scale bar represents 2 μm.
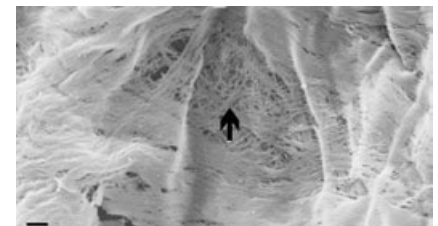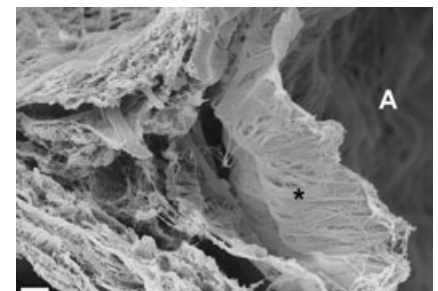

FIG. 7. Higher magnification of Fig. 4b showing a partly detached and everted luminal sheet (asterisk) lining the empty acinar space (A). Note the thin meshwork of fibrils (asterisk), measuring 77–115 nm, just under the smoother layer that faces the empty space. Original ×3500; the scale bar represents 6 μm.

Typical basement membranes are usually described as having three major layers. The one just under the epithelium is the lamina lucida, which is followed by the lamina densa and last by a less well delimited pars fibroreticularis [26]. SEM preparations to visualize tracheal or bronchial basement membranes reveal that, once epithelial cells are gently removed, as with EDTA, the lamina densa appears as a mostly homogeneous and smooth sheet [27,28]. Just under this layer there is the more heterogeneous pars fibroreticularis, which contains layers of collagenous fibres in varying degrees of organization. Our images show that the stromal component directly facing the acinar lumen consists of distinct connective tissue fibrils in a parallel arrangement, which is markedly different from the lamina densa morphology as seen under SEM. We therefore assume that the comparatively less resistant components of the lamina densa, such as collagen IV, were removed by the alkali treatment, leaving exposed the underlying pars fibroreticularis. Indeed, a recent investigation showed that current processing methods, including de-cellularization, aimed at producing a purified ECM, rarely result in an intact basement membrane [29].

The present results also showed that just under the luminal fibrous sheet there is a meshwork composed of less organized connective tissue fibres, which should also be part of the pars fibroreticularis. The composition and structure of the pars fibroreticularis is more variable than that of other parts of the basement membrane [30], and differences have been found among tissues. For example, in the rat skin, a less organized meshwork of fibres follows immediately after the lamina densa [28], whereas in the rat trachea there is first a sheet of fibres in parallel arrangement and then a layer of fibres running in various directions [27]. This latter disposition of the pars fibroreticularis is similar to what we found in the human prostate. However, in the rat trachea the parallel collagen fibres making up the fibrous sheet under the lamina densa are thicker, at 500 nm on average, while in the prostate these fibres were 115–154 nm thick. This difference might be explained as a functional adaptation, as prostate acini and ducts are subjected to less stretching forces than the trachea. This finding also confirms previous data which showed that the pars fibroreticularis is structurally more variable than other regions of basement membranes [30].

In conclusion, our results show that, in the TZ of the human prostate, dense stromal fibrous components around acini act as a diffusion barrier that might enhance local cellular responses and events that are known to occur in disorders such as BPH. The periacinar stroma also includes a distinct pars fibroreticularis, and this supports the notion of high structural variability in this region of basement membranes.

CONFLICT OF INTEREST

None declared.

REFERENCES

1 **McNeal JE.** Anatomy of the prostate and morphogenesis of BPH. *Prog Clin Biol Res* 1984; **145**: 27–53
2 **Wei JT, Calhoun E, Jacobsen SJ.** Urologic diseases in America project: benign prostatic hyperplasia. *J Urol* 2005; **173**: 1256–61
3 **Doll JA, Reiher FK, Crawford SE, Pins MR, Campbell SC, Bouck NP.** Thrombospondin-1, vascular endothelial growth factor and fibroblast growth factor-2 are key functional regulators of angiogenesis in the prostate. *Prostate* 2001; **49**: 293–305
4 **Cunha GR.** Role of mesenchymal–epithelial interactions in normal and abnormal development of mammary gland and prostate. *Cancer* 1994; **74**: 1030–44
5 **Nagle RB.** Role of the extracellular matrix in prostate carcinogenesis. *J Cell Biochem* 2004; **91**: 36–40
6 **Sakai I, Harada K, Hara I, Eto H, Miyake H.** A comparison of the biological features between prostate cancers arising in the transition and peripheral zones. *BJU Int* 2005; **96**: 528–32
7 **Terry DE, Clark AF.** Glycosaminoglycans in the three lobes of the rat prostate following castration and testosterone treatment. *Biochem Cell Biol* 1996; **74**: 653–8
8 **Li SC, Chen GF, Chan PS, Choi HL, Ho SM, Chan FL.** Altered expression of extracellular matrix and proteinases in Noble rat prostate gland after long-term treatment with sex steroids. *Prostate* 2001; **49**: 58–71
9 **Srodon M, Epstein JI.** Central zone histology of the prostate: a mimicker of high-grade prostatic intraepithelial neoplasia. *Hum Pathol* 2002; **33**: 518–23
10 **Cardoso LE, Falcao PG, Sampaio FJ.** Increased and localized accumulation of chondroitin sulphate proteoglycans in the hyperplastic human prostate. *BJU Int* 2004; **93**: 532–8
11 **Costa WS, De Carvalho AM, Babinski MA, Chagas MA, Sampaio FJB.** Volumetric density of elastic and reticular fibers in transition zone of controls and patients with benign prostatic hyperplasia. *Urology* 2004; **64**: 693–7
12 **Glynne–Jones E, Harper ME, Seery LT et al.** TENB2, a proteoglycan identified in prostate cancer that is associated with disease progression and androgen independence. *Int J Cancer* 2001; **94**: 178–84
13 **Savore C, Zhang C, Muir C et al.** Perlecan knockdown in metastatic prostate cancer cells reduces heparin-binding growth factor responses in vitro and tumor growth in vivo. *Clin Exp Metastasis* 2005; **22**: 377–90
14 **Heatfield BM, Sanefuji H, Trump BF.** Studies on carcinogenesis of human prostate. III. Long-term explant culture of normal prostate and benign prostatic hyperplasia: transmission and scanning electron microscopy. *J Natl Cancer Inst* 1982; **69**: 757–66
15 **Morrison C, Thornhill J, Gaffney E.** The connective tissue framework in the normal prostate, BPH & prostate cancer: analysis by scanning electron microscopy after cellular digestion. *Urol Res* 2000; **28**: 304–7
16 **Babinski MA, Chagas MA, Costa WS, Sampaio FJB.** Prostatic epithelial and luminal area in the transition zone acini: morphometric analysis in normal and hyperplastic human prostate. *BJU Int* 2003; **92**: 592–6
17 **Ohtani O.** Three-dimensional organization of the collagen fibrillar

framework of the human and rat livers. *Arch Histol Cytol* 1988; **51**: 473–88

18 Byun SS, Jeong H, Jo MK, Lee E. Relative proportions of tissue components in the prostate: are they related to the development of symptomatic BPH in Korean men? *Urology* 2005; **66**: 593–6

19 Goo YA, Goodlett DR, Pascal LE *et al.* Stromal mesenchyme cell genes of the human prostate and bladder. *BMC Urol* 2005; **5**: 17

20 Aboseif S, El–Sakka A, Young P, Cunha G. Mesenchymal reprogramming of adult human epithelial differentiation. *Differentiation* 1999; **65**: 113–8

21 Akashi T, Minami J, Ishige Y *et al.* Basement membrane matrix modifies cytokine interactions between lung cancer cells and fibroblasts. *Pathobiology* 2005; **72**: 250–9

22 Royuela M, Ricote M, Parsons MS, Garcia–Tunon I, Paniagua R, de Miguel MP. Immunohistochemical analysis of the IL-6 family of cytokines and their receptors in benign, hyperplasic, and malignant human prostate. *J Pathol* 2004; **202**: 41–9

23 Suzuki K, Obara K, Kobayashi K *et al.* Role of connective tissue growth factor in fibronectin synthesis in cultured human prostate stromal cells. *Urology* 2006; **67**: 647–53

24 Zaman MH, Trapani LM, Sieminski AL *et al.* Migration of tumor cells in 3D matrices is governed by matrix stiffness along with cell-matrix adhesion and proteolysis. *Proc Natl Acad Sci USA* 2006; **103**: 10889–94

25 Pradhan BK, Chandra K. Morphogenesis of nodular hyperplasia-prostate. *J Urol* 1975; **113**: 210–3

26 Lindblom A, Paulsson M. Basement membranes. In: Comper WD ed. *Extracellular Matrix* Vol. 1. The Netherlands: Harwood Academic Publishers, 1996

27 Evans MJ, Van Winkle LS, Fanucchi MV *et al.* Three-dimensional organization of the lamina reticularis in the rat tracheal basement membrane zone. *Am J Respir Cell Mol Biol* 2000; **22**: 393–7

28 Osawa T, Feng XY, Nozaka Y. Scanning electron microscopic observations of the basement membranes with dithiothreitol separation. *Med Electron Microsc* 2003; **36**: 132–8

29 Brown B, Lindberg K, Reing J, Stolz DB, Badylak SF. The basement membrane component of biologic scaffolds derived from extracellular matrix. *Tissue Eng* 2006; **12**: 519–26

30 Merker HJ. Morphology of the basement membrane. *Microsc Res Tech* 1994; **28**: 95–124

Correspondence: Luiz E.M. Cardoso, Urogenital Research Unit – UERJ, Avenue. 28 de Setembro, 87 – fundos – FCM – térreo, Rio de Janeiro, RJ, 20551–030, Brazil. e-mail: luizemcardoso@gmail.com

Abbreviations: **TZ**, transition zone; **ECM**, extracellular matrix; **SEM**, scanning electron microscopy.